VHF OSCILLATIONS IN A PENNING GAUGE

A Thesis

Presented to

The Faculty of the Department of Physics

The College of William and Mary in Virginia

In Partial Fulfillment

Of the Requirements for the Degree of

Master of Arts

By

Robert Newman Dennis, Jr.

May 1962

APPROVAL SHEET

This thesis is submitted in partial fulfillment of

the requirements for the degree of

Master of Arts

Robert N. Dennis Jr.

Author

Approved, May 1962:

Frederic R. Crownfield Jr.

Frederic R. Crownfield, Jr., Ph.D.

John L. McKnight

John L. McKnight, Ph.D.

James D. Lawrence Jr.

James D. Lawrence, Jr., Ph.D.

D.E. McLennan

Gul Crawford

Robert L. Kernell

R.E. Smith

John H. Long

ACKNOWLEDGMENTS

The writer wishes to express his appreciation to Professor Frederic R. Crownfield, Jr., under whose guidence this investigation was conducted, for his patient guidence and helpful criticism throughout the investigation. The author is also indebted to the staff of the William and Mary physics department for their advice on research methods, and particularly, to Professor John L. McKnight and Professor James D. Lawrence for their careful reading and criticism of the manuscript. The author's wife, Carolin Dennis, deserves special thanks for her patience in helping to prepare the manuscript. This investigation was supported by the National Aeronautics and Space Administration under grant number NsG-106-61.

TABLE OF CONTENTS

	Page
ACKNOWLEDGMENTS	iii
LIST OF FIGURES AND TABLES.	v
ABSTRACT.	vi
INTRODUCTION.	2
THE PENNING GAUGE	4
ELECTROMAGNETIC MODES IN A PLASMA FILLED CYLINDRICAL CAVITY IN AN EXTERNAL UNIFORM MAGNETIC FIELD	7
EQUIPMENT	17
PROCEDURE AND DATA.	28
EXPERIMENTAL RESULTS AND CONCLUSIONS.	32
SUMMARY	34
BIBLIOGRAPHY.	36

LIST OF FIGURES AND TABLES

Page

PLOT OF SLOW WAVE DISPERSION RELATION AND EXPERIMENTAL DATA. 16

BLOCK DIAGRAM OF EXPERIMENTAL APPARATUS. 18

PENNING GAUGE. 19

HIGH VACUUM SYSTEM 21

HIGH VOLTAGE POWER SUPPLY. 24

SUMMARY OF EXPERIMENTAL DATA 29

ABSTRACT

VHF oscillations with well defined frequencies have been observed using a receiver connected to the anode of a Penning ion gauge. These oscillations seem to be associated with the slow wave modes of a plasma filled conducting cylinder. Slight variations in voltage cause abrupt changes in the gauge current concurrent with changes in the amplitude and breadth of observed resonances. This relation suggests that these slow waves may help to account for the gauge current. It appears that the slow wave modes are excited by a beam plasma interaction between electrons oscillating in the electrostatic potential well between the cathodes and the plasma.

INTRODUCTION

The Penning gauge has found a great deal of application in the measurement of pressure in vacuum systems, as an ion source, and as a plasma source. The qualitative behavior of the gas discharge occurring in such a gauge is well understood, but a detailed theory has never been given; in fact, the descriptions of various phenomena occurring in the gauge given by different authors seem to be contradictory. Among the processes which are believed to occur are two-beam instability and plasma turbulence. This has given the discharge a reputation among plasma physicists as being very "dirty".

The present work describes oscillations which have been discovered and measured in a Penning gauge under certain conditions of operation. The observed phenomena indicate that these oscillations correspond to the slow-waves in a plasma filled cylinder which have been discussed by earlier authors, and that they are probably excited by the interaction between the oscillating electrons (electron beams) and the plasma in the gauge.

A derivation is given of the dielectric constant tensor for a plasma in a magnetic field, and this is used to find the possible frequencies of oscillation of a plasma filled cylindrical cavity for various plasma densities. The frequencies of the oscillations observed in the gauge used for this work can be unambiguously assigned to the lowest three modes of oscillation predicted by the theory, and correlations between the gauge current and the behavior of the observed oscillations indicate that they are associated with the conduction mechanism of the discharge.

THE PENNING GAUGE

The Penning gauge[1] was originally proposed as a device for the measurement of pressure in a vacuum system. It has since found use as an ion source for particle accelerators and mass spectrometers[2] and as a plasma source[3] for various experiments. The gauge is ordinarily used at pressures such that the mean free path of electrons is larger than the dimensions of the gauge tube. Electrons in the discharge are prevented from reaching the walls of the gauge by a combination of electric and magnetic fields. The Penning gauge is particularly convenient for vacuum measurement because the current drawn by the gauge over a large range of pressures is proportional to the pressure as in other ionization gauges,[4] but without the necessity of a hot cathode to maintain the current.

The basic gauge consists of an anode placed between

---

[1] F. M. Penning, Physica 4, 71 (1937).

[2] P. C. Thonemann, Progress in Nuclear Physics, ed. O. R. Frisch, (Pergamon Press Ltd., London, 1953), Vol. 3 Chap. 8.

[3] J. E. Drummond, Plasma Physics (McGraw-Hill Book Company, Inc., New York, 1961) Chap. 12.

[4] K. M. Simpson, High Vacuum Equipment and Technique ed. A. Guthrie and R. K. Wakerling, (McGraw-Hill Book Company, Inc., New York, 1949), 1st ed., Chap. 3.

two cathodes. The electrodes are arranged in a plane parallel geometry with a spacing between cathodes of a few centimeters. The anode, which is spaced midway between the cathodes, is reduced to a simple ring of wire to allow the electrons in the tube to pass through. In operation, a constant magnetic field is applied perpendicular to the planes of the electrodes. A high potential difference is applied between the anode ring and the cathodes. The resulting configuration of fields produces a maximum of the electrostatic potential near the anode, so that the electrons tend to be trapped in a potential well. The magnetic field causes them to spiral about the direction of the field, preventing them from reaching the sides of the tube. In this manner, the electrons remain in the discharge long enough to provide sufficient ionization for the operation of the gauge.

While the qualitative description of the operation of a Penning gauge as described above is well understood, no detailed theory has been worked out. Backus[5] states that the gauge current was larger than that expected from collision scattering theory but did not offer a quantitative explanation for the excess current. Knauer[6] examined the dis-

---

[5] J. Backus, Characteristics of Electrical Discharges in Magnetic Fields, eds. A. Guthrie and R. K. Wakerling (McGraw-Hill Book Company, Inc., New York, 1949), Chap. 11.

[6] W. Knauer, Hughes Res. Rep. 222 (1961).

charge mechanism in restricted ranges of pressure and magnetic fields and proposed a mechanism by which the gauge current observed could be estimated from well known diffusion theory.[7] However, the results of Knauer[6] and Salz, et al,[8] show a contrast in that Knauer believes that most of the potential drop occurs near the anode, while Salz and his group observed most of the drop to be near the cathode; a difference in geometry used in these two investigations may account for the difference. The lack of a theory of the discharge mechanism has given this kind of discharge the reputation of being "dirty". This reputation is primarily the result of the fact that there is no detailed theory of the mechanisms by which charged particles cross the magnetic field lines and of the fact that the oscillating electrons in the gauge act as particle beams -- a configuration known to be unstable.[9]

---

[7] S. Chandrasekhar, Plasma Physics, comp. by S. K. Trehan (The University of Chicago Press, Chicago, 1961), 3rd ed., Chap. 7.

[8] F. Salz, R. G. Meyerand, Jr., E. C. Lary, and A. P. Walsh, Phys. Rev. Letters 6, 523 (1961).

[9] D. Bohm and E. P. Gross, Phys. Rev. 75, 1851, 1864 (1949) and Phys. Rev. 79, 992 (1950).

ELECTROMAGNETIC MODES IN A PLASMA FILLED CYLINDRICAL CAVITY IN AN EXTERNAL UNIFORM MAGNETIC FIELD

Trivelpiece and Gould[10] have developed the theory of space charge waves in a uniform plasma contained in a cylindrical wave guide with an applied homogeneous magnetic field. Their approach will be used to derive a dispersion relation for the corresponding modes of oscillation of a plasma filled cylindrical cavity. First the dielectric tensor for a uniform plasma in a homogeneous magnetic field will be obtained.

In general, a magnetized plasma is anisotropic and the relation between the electric displacement $\vec{D}$ and the electric field $\vec{E}$ requires a tensor for the dielectric constant ϵ. The electric displacement $\vec{D}$ can be written in terms of the polarization $\vec{P}$ or the dielectric constant tensor $\underline{\underline{\epsilon}}$ as

$$\vec{D} = \epsilon_0 \vec{E} + \vec{P} = \underline{\underline{\epsilon}} \cdot \vec{E}.$$

The polarization $\vec{P}$ may be written as $\vec{P} = nq\vec{r}$, where $q\vec{r}$ is the induced dipole moment due to one particle and n is the number of particles per unit volume. Using this expression for $\vec{P}$ the tensor relation can be expanded in component

---

[10] A. W. Trivelpiece and R. W. Gould, J. Appl. Phys. 30, 1784 (1959).

form as

$$\sum_j \epsilon_{ij} \vec{E}_j = -ne\vec{r}_i + \epsilon_o \vec{E}_i \ , \qquad (1)$$

where q has been set equal to -e for electrons. The motion of ions has been neglected because their mass is large in comparison to the electron mass. Hence their acceleration due to the fields is relatively small.

Following Trivelpiece and Gould,[10] all quantities will be assumed to have a harmonic time dependent perturbation added to an average steady state term, thus

$$\vec{E} = \vec{E}_o + \vec{E} e^{i\omega t} \qquad (2)$$

$$\vec{\rho} = \vec{\rho}_o + \vec{r} e^{i\omega t} , \qquad (3)$$

where $\vec{\rho}$ is the position vector of the particle. It is assumed that the force on the electrons due to the magnetic field component of the wave is much smaller than that due to the electric force, since $\frac{v}{c} \ll 1$. Taking $\vec{B}_o$, the applied magnetic field, along the z axis of the cylindrical coordinate system the components of the Lorentz force equation for electrons,

$$m\ddot{\vec{\rho}} = -e[\vec{E} + \dot{\vec{\rho}} \times \vec{B}_o] ,$$

are

$$\omega^2 m \vec{r}_r = e[\vec{E}_r - i\omega\vec{r}_\theta \vec{B}_o] \qquad (4)$$

$$\omega^2 m \vec{r}_\theta = e[\vec{E}_\theta + i\omega\vec{r}_r \vec{B}_o] \qquad (5)$$

$$\omega^2 m \vec{r}_z = e[\vec{E}_z] . \qquad (6)$$

Substituting Eq. (5) into Eq. (4) and solving for $\vec{r}_r$ gives

$$\vec{r}_r = -\frac{e}{m}\left[\frac{\omega\vec{E}_r - i\omega_c\vec{E}_\theta}{\omega(\omega_c^2 - \omega^2)}\right] . \qquad (7)$$

Using Eq. (4) in Eq. (5) and solving for $\vec{r}_\theta$ gives

$$\vec{r}_\theta = -\frac{e}{m}\left[\frac{\omega\vec{E}_\theta + i\omega_c\vec{E}_r}{\omega(\omega_c^2-\omega^2)}\right], \tag{8}$$

where ω_c is the cyclotron radian frequency,

$$\omega_c = \frac{e}{m}B_o . \tag{9}$$

Equation (6) can be rewritten as

$$\vec{r}_z = \frac{e}{m\omega^2}\vec{E}_z . \tag{10}$$

Equation (1) can now be used to solve for the components of the dielectric tensor. The radical component of $\vec{D}$ is

$$\vec{D}_r = \epsilon_{rr}\vec{E}_r + \epsilon_{r\theta}\vec{E}_\theta + \epsilon_{rz}\vec{E}_z = -ne\vec{r}_r + \epsilon_o\vec{E}_r .$$

Substitution of Eq. (7) for $\vec{r}_r$ results in

$$\epsilon_{rr}\vec{E}_r + \epsilon_{r\theta}\vec{E}_\theta + \epsilon_{rz}\vec{E}_z = \frac{ne^2}{m}\left[\frac{\omega\vec{E}_r - i\omega_c\vec{E}_\theta}{\omega(\omega_c^2-\omega^2)}\right] + \epsilon_o\vec{E}_r . \tag{11}$$

Equating coefficients of the components of the electric field appearing on both sides of Eq. (11) yields three components of the dielectric tensor;

$$\frac{\epsilon_{rr}}{\epsilon_o} = 1 + \frac{\omega_p^2}{\omega_c^2 - \omega^2} \tag{12}$$

$$\frac{j\epsilon_{r\theta}}{\epsilon_o} = \frac{\omega_c}{\omega} \frac{\omega_p^2}{\omega_c^2 - \omega^2} \tag{13}$$

$$\epsilon_{rz} = 0 \quad ,$$

where ω_p is the electron plasma radian frequency given by

$$\omega_p^2 = \frac{ne^2}{m\epsilon_o} \quad .$$

The azimuthal component of $\vec{D}$ is written

$$\vec{D}_\theta = \epsilon_{\theta r}\vec{E}_r + \epsilon_{\theta\theta}\vec{E}_\theta + \epsilon_{\theta z}\vec{E}_z = -ne\vec{r}_\theta + \epsilon_o\vec{E}_\theta$$

or upon substitution of Eq. (8) for $\vec{r}_\theta$,

$$\epsilon_{\theta r}\vec{E}_r + \epsilon_{\theta\theta}\vec{E}_\theta + \epsilon_{\theta z}\vec{E}_z = \frac{ne^2}{m}\left[\frac{\omega\vec{E}_\theta + j\omega_c\vec{E}_r}{\omega(\omega_c^2 - \omega^2)}\right] + \epsilon_o\vec{E}_\theta \; . \tag{14}$$

Again, equating coefficients of the electric field appearing on both sides of Eq. (14) gives three additional components of the dielectric tensor;

$$\frac{\epsilon_{\theta\theta}}{\epsilon_o} = 1 + \frac{\omega_p^2}{\omega_c^2 - \omega^2} \tag{15}$$

$$\frac{-j\epsilon_{\theta r}}{\epsilon_o} = \frac{\omega_c}{\omega} \frac{\omega_p^2}{\omega_c^2 - \omega^2} \tag{16}$$

$$\epsilon_{\theta z} = 0 \quad .$$

The axial component of $\vec{D}$

$$\vec{D}_z = \epsilon_{zr}\vec{E}_r + \epsilon_{z\theta}\vec{E}_\theta + \epsilon_{zz}\vec{E}_z = -ne\vec{r}_z + \epsilon_o\vec{E}_z$$

can be rewritten using Eq. (10) for $\vec{r}_z$ as

$$\epsilon_{zr}\vec{E}_r + \epsilon_{z\theta}\vec{E}_\theta + \epsilon_{zz}\vec{E}_z = -\frac{ne^2}{m}\vec{E}_z + \epsilon_o\vec{E}_z \ . \tag{17}$$

Equating coefficients of the electric field components as done above gives the remaining three components of the dielectric tensor as

$$\frac{\epsilon_{zz}}{\epsilon_o} = 1 - \frac{\omega_p^2}{\omega^2} \tag{18}$$

$$\epsilon_{zr} = \epsilon_{z\theta} = 0 \ .$$

Using the components given above, the dielectric tensor can be written

$$\underline{\underline{\epsilon}} = \epsilon_o \begin{vmatrix} \epsilon_1 & i\epsilon_2 & 0 \\ -i\epsilon_2 & \epsilon_1 & 0 \\ 0 & 0 & \epsilon_3 \end{vmatrix} , \tag{19}$$

where

$$\epsilon_o\epsilon_1 = \epsilon_{rr} = \epsilon_{\theta\theta}$$

$$i\epsilon_o\epsilon_2 = -\epsilon_{\theta r} = \epsilon_{r\theta}$$

$$\epsilon_o\epsilon_3 = \epsilon_{zz} \ .$$

Using the dielectric tensor, the dispersion relation for slow wave modes in a cylindrical cavity of radius "a" and height "h" filled with a uniform plasma and placed in a homogeneous magnetic field will now be derived. Using the quasi-static approximation of reference 10, the electric field may be derived from a scalar potential alone, thus

$$\vec{E} = -\nabla \phi$$

The response of the plasma to the electric field is contained in the dielectric tensor, hence from the Maxwell equation,

$$\nabla \cdot \vec{D} = 0$$

one obtains

$$\nabla \cdot \underline{\underline{\epsilon}} \cdot \vec{E} = \nabla \cdot \underline{\underline{\epsilon}} \cdot \nabla \phi = 0 \qquad (20)$$

Equation (20) can be written in cylindrical coordinates as

$$\nabla \cdot \underline{\underline{\epsilon}} \cdot \nabla \phi = \frac{1}{r} \frac{\partial}{\partial r}\left[\epsilon_1 r \frac{\partial \phi}{\partial r} + i\epsilon_2 \frac{\partial \phi}{\partial \theta}\right] + \frac{1}{r} \frac{\partial}{\partial \theta}\left[\epsilon_1 \frac{1}{r} \frac{\partial \phi}{\partial \theta} - i\epsilon_2 \frac{\partial \phi}{\partial r}\right] + \frac{\partial}{\partial z} \epsilon_3 \frac{\partial \phi}{\partial z} = 0 . \qquad (21)$$

Dividing Eq. (21) by ϵ_1 and performing the indicated operations results in the expression

$$\frac{\partial^2 \phi}{\partial r^2} + \frac{1}{r}\frac{\partial \phi}{\partial r} + \frac{1}{r^2}\frac{\partial^2 \phi}{\partial \theta^2} + \frac{\epsilon_3}{\epsilon_1}\frac{\partial^2 \phi}{\partial z^2} = 0 . \qquad (22)$$

If a solution of the form

$$\phi = R(r)\,\Theta(\theta)\,Z(z)$$

is substituted in Eq. (22) the equation

$$\Theta Z R'' + \frac{1}{r}\Theta Z R' + \frac{1}{r^2} R Z \Theta'' + \frac{\epsilon_3}{\epsilon_1} R \Theta Z'' = 0$$

results. Division by $R\,\Theta\,Z$ leaves

$$\frac{R''}{R} + \frac{1}{r}\frac{R'}{R} + \frac{1}{r^2}\frac{\Theta''}{\Theta} + \frac{\epsilon_3}{\epsilon_1}\frac{Z''}{Z} = 0 . \qquad (23)$$

From this it can be seen that $\frac{Z''}{Z}$ is independent of the two other variables and can be set equal to a constant, therefore let

$$\frac{Z''}{Z} = -K^2$$

which has a solution

$$Z = C_1 \sin(Kz) + C' \cos(Kz) .$$

Choosing

$$Z = c_1 \sin(K_m z)$$

with

$$K_m = \frac{m\pi}{h}, \qquad (m = \text{integer}), \tag{24}$$

satisfies the boundary condition that the potential vanish at the ends of the cylinder, i.e., z = 0, z = h. Replacing $\frac{Z''}{Z}$ by $-K_m^2$ and multiplying by r^2 puts Eq. (23) in the form

$$r^2 \frac{R''}{R} + r\frac{R'}{R} + \frac{\Theta''}{\Theta} - \frac{\epsilon_3}{\epsilon_1} K_m^2 r^2 = 0 \tag{25}$$

Setting $\frac{\Theta''}{\Theta}$ equal to a constant one has

$$\frac{\Theta''}{\Theta} = -n^2$$

with a solution

$$\Theta = c_2 e^{in\theta}, \tag{26}$$

which is single valued if $n = \pm$ integer.

Upon replacing $\frac{\Theta''}{\Theta}$ by $-n^2$ in Eq. (25) the equation

$$r^2 \frac{R''}{R} + r\frac{R'}{R} - \left(n^2 + \frac{\epsilon_3}{\epsilon_1} K_m^2 r^2\right) = 0 \tag{27}$$

is obtained. After making the substitution

$$T^2 = -K_m^2 \frac{\epsilon_3}{\epsilon_1} = -K_m^2 \left[\frac{1 - \frac{\omega_p^2}{\omega^2}}{1 + \frac{\omega_p^2}{\omega_c^2 - \omega^2}}\right] \tag{28}$$

and multiplying Eq. (27) by R the Bessel equation

$$r^2 R'' + r R' + (T^2 r^2 - n^2) R = 0$$

in the radial component results. The solution to this equation which is finite at $r = 0$ is

$$R = C_3 J_n(Tr) \qquad 0 \leq r \leq a. \qquad (29)$$

The solution for the potential can now be written

$$\Phi = B_{\pm} J_n(Tr) \sin(K_m z) e^{jn\theta},$$

where $B_{\pm} = C_1 C_2 C_3$. Since the cavity is assumed to be a perfect conductor, the potential must vanish at the walls. This has been satisfied for $z = 0, h$ by the choice of $K_m = \frac{m\pi}{h}$. The radial boundary condition requires that

$$J_n(Ta) = 0$$

or

$$Ta = p_{n\ell}, \qquad (30)$$

where $p_{n\ell}$ is the ℓ^{th} zero of the n^{th} Bessel function of the first kind. Substitution of Eq. (28) for T into Eq. (30) gives after solving for $k_m a/p_{n\ell}$

$$A \equiv \frac{K_m a}{p_{n\ell}} = \pm \left[\frac{\omega^2(\omega_c^2 + \omega_p^2 - \omega^2)}{(\omega_p^2 - \omega^2)(\omega_c^2 - \omega^2)} \right]^{\frac{1}{2}} \qquad (31)$$

which is the desired dispersion relation for slow waves in a cylindrical cavity. This is plotted in Fig. (1), where $F = \omega/\omega_c$ is shown as a function of A for various values of $P = \omega_p/\omega_c$.

FIGURE 1

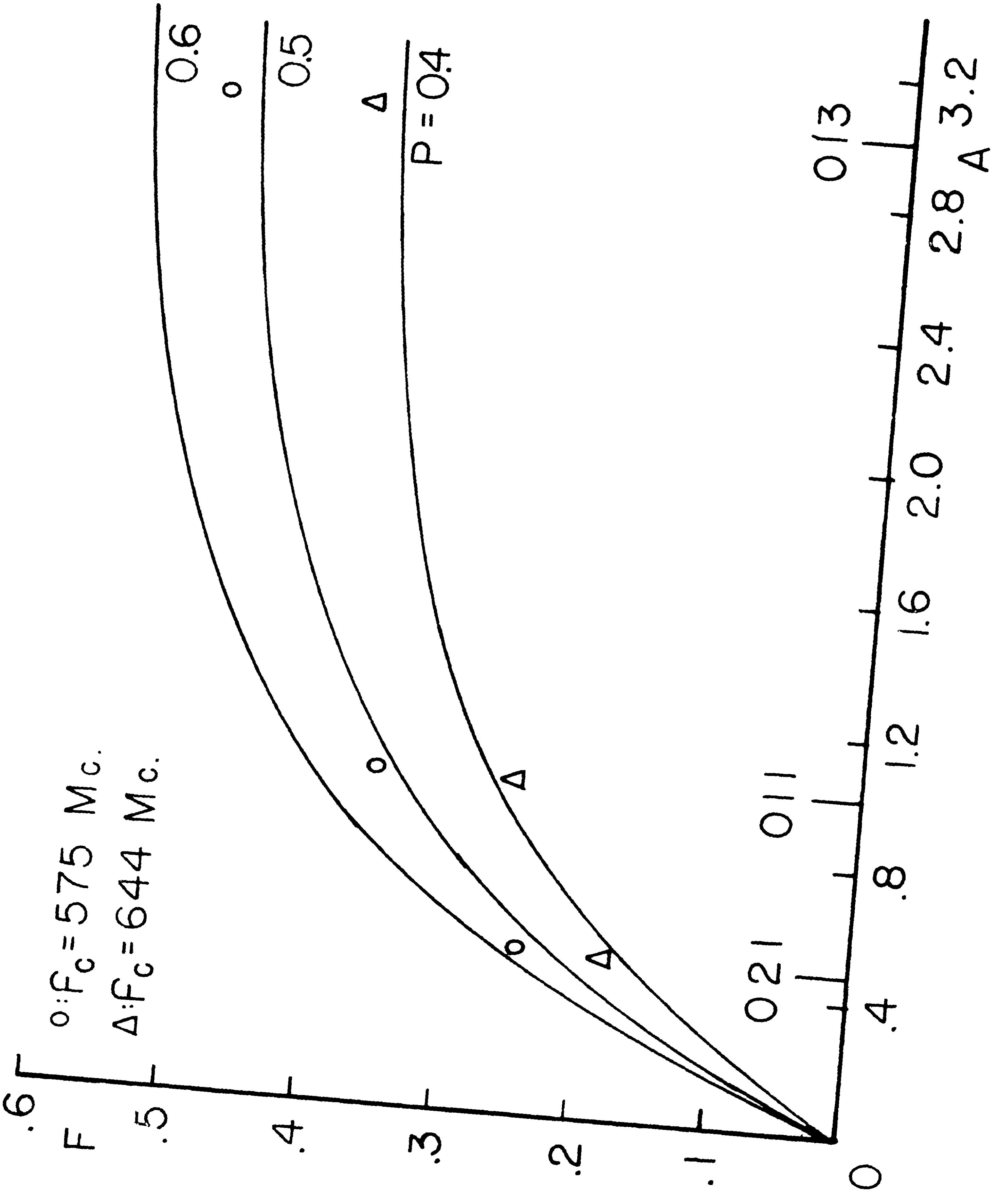
o: F_c = 575 Mc.
Δ: F_c = 644 Mc.
F
A
P = 0.4
0.5
0.6
021
011
013
0
.1
.2
.3
.4
.5
.6
.4
.8
1.2
1.6
2.0
2.4
2.8
3.2

EQUIPMENT

A block diagram of the equipment is shown in Fig. 2. The Penning gauge as used in the experiment was provided with both an adjustable high voltage source and a variable magnetic field. In addition to the high vacuum system evacuating the gauge cavity, a controlled leak is used to maintain the gauge pressure at a uniform value. The oscillations in the cavity are detected by a tunable high frequency receiver the output of which is displayed on a panoramic adaptor.

A full scale drawing showing front and side views of the gauge construction used for the present work is shown in Fig. 3. The gauge tube is a right circular cylinder of copper 4 cm long and 6.2 cm ID. The caps over the ends of the cylinder are made of brass and are soldered directly to the cylinder. The anode is a circular ring of #17 AWG copper wire 3 cm in diameter. A lead, also made with #17 AWG copper wire, is soldered to the anode ring. This lead is brought out of the cavity through a 12.7 cm length of 1.25 cm ID copper tubing. The lead is centered within the copper tube by a 10 cm length of 4 mm glass tubing supported by perforated teflon spacers at each end of the copper tube. The anode lead is brought

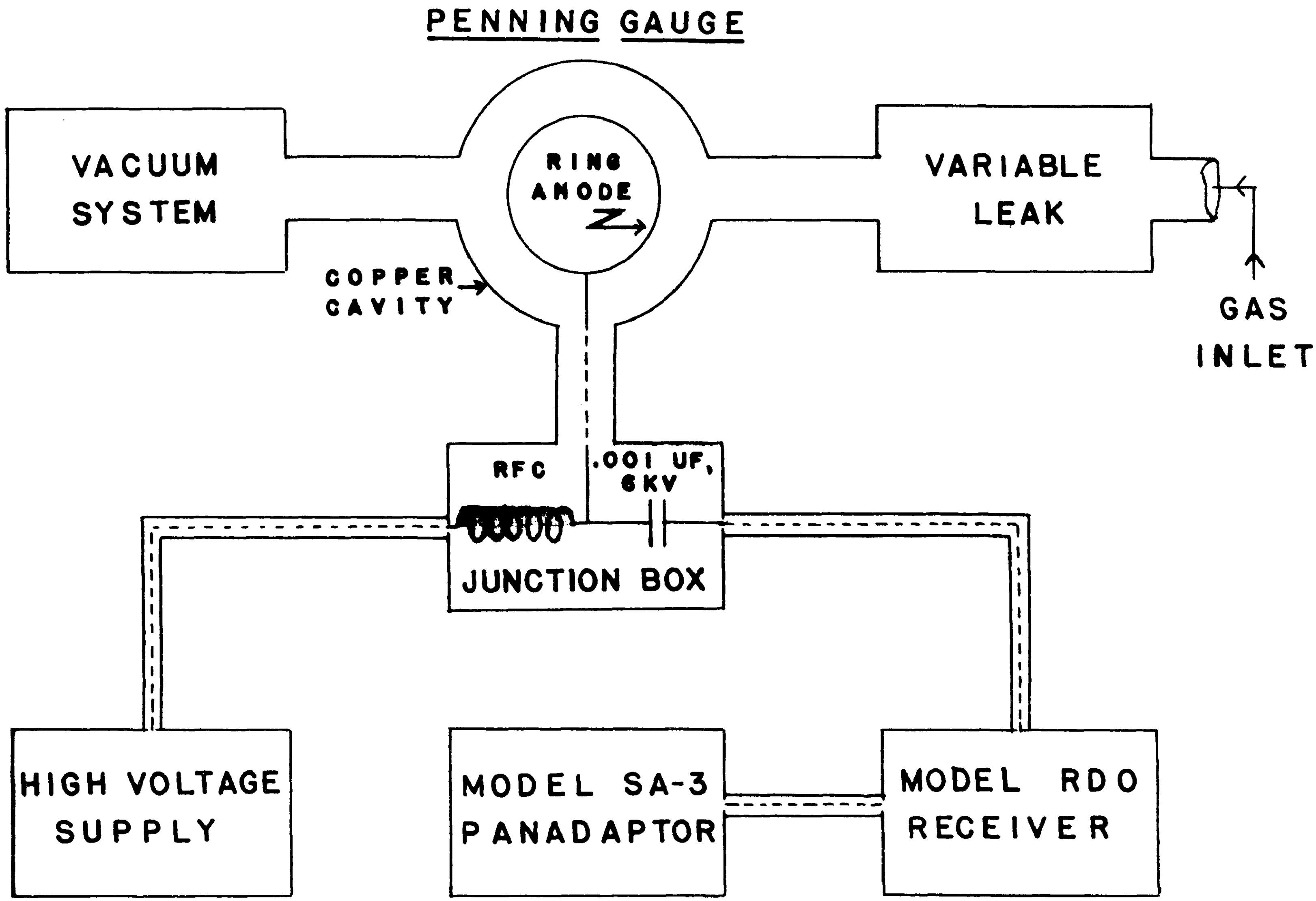

FIG. 2

BLOCK DIAGRAM OF EXPERIMENTAL APPARATUS

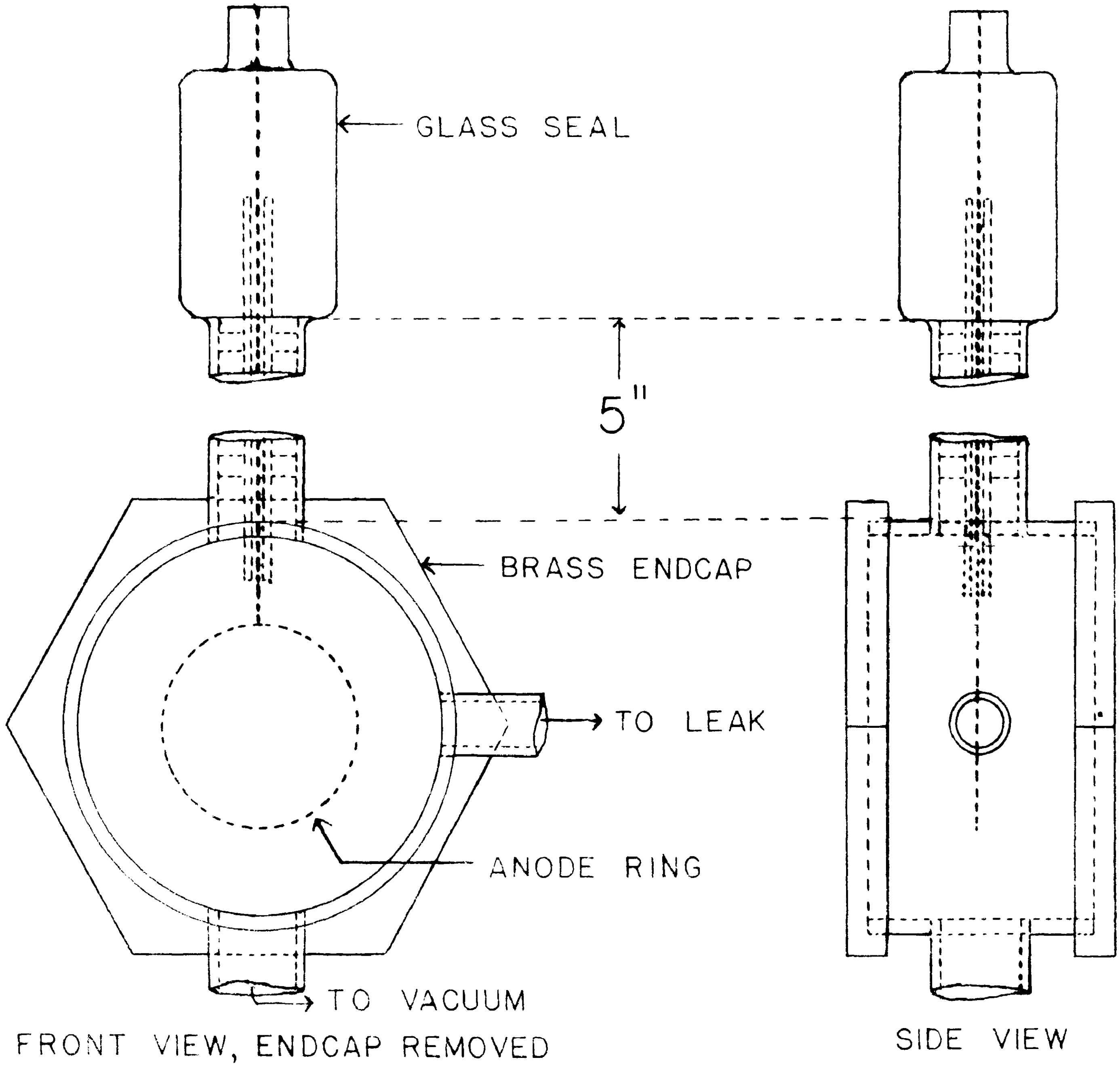

FIG.3, PENNING GAUGE, SCALE 1:1

through the glass tubing from the anode ring to a metal-to-glass seal mounted on the opposite end of the copper tube. This metal-to-glass seal insulates the anode lead from the copper tube which is at cathode potential.

As mentioned in reference 4, sputtering of cathode material onto the anode lead insulation may provide a current path which shunts the circuit between anode and cathode through the discharge, giving misleading indications of the current drawn by the gauge. This sputtering can be minimized by preventing ionization in the region of the glass seal. If the seal is kept out of the magnetic field, electrons will not be prevented from reaching the anode lead by the magnetic field. Since the mean free path is much greater than the seal dimensions, there will be little ionization by collisions in the short distance between the copper tube and the anode lead. Consequently sputtering by ions will be slight.

The magnetic field is supplied by a Harvey-Wells type L-128 electromagnet and HS-1050 magnet power supply. The magnetic field strength is variable from 0 to 12.5 kilogauss in a two inch gap between twelve inch diameter pole faces.

Figure 4 shows a diagram of the vacuum system. A 2 inch Veeco model EP 2-AB air cooled oil diffusion pump backed by a Welch model 1405-H mechanical pump provides the high vacuum. The high vacuum side of the diffusion pump is connected to an 11 inch copper tube 2.5 inches ID

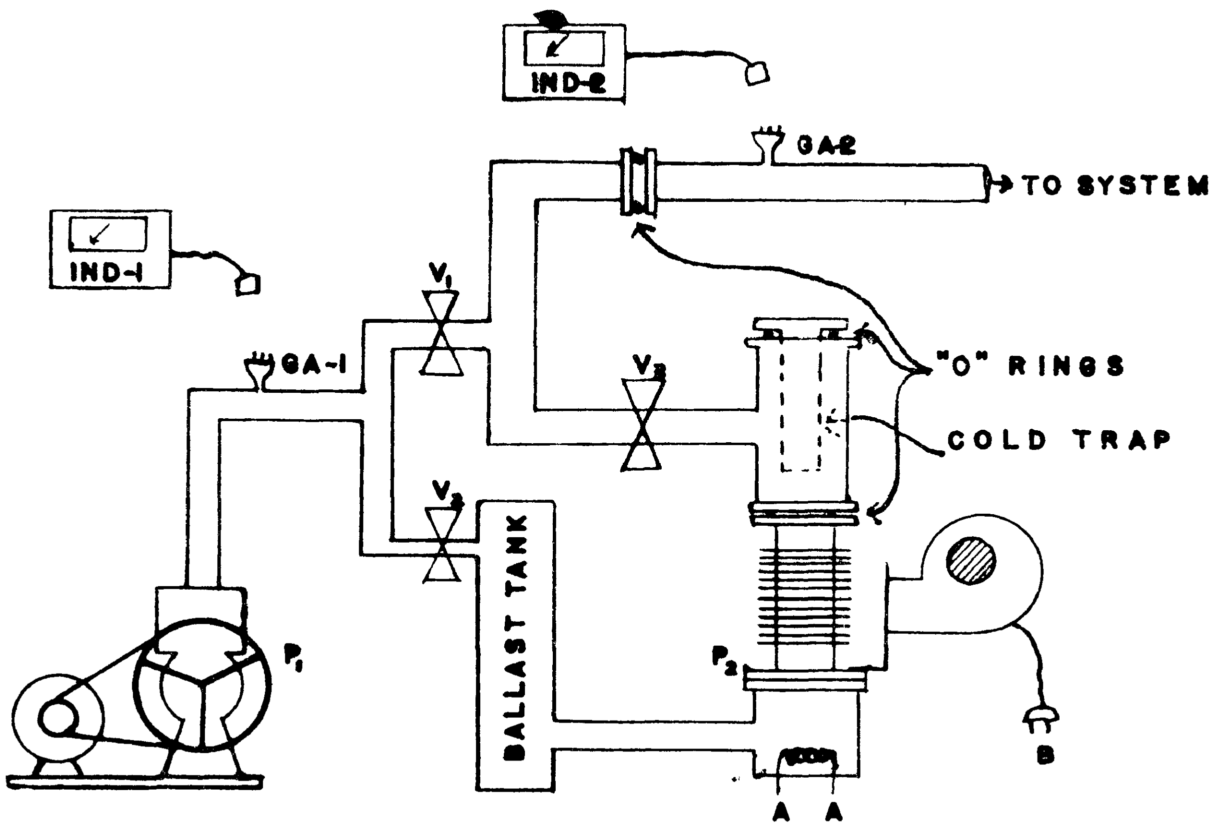

P_1 ; WELCH MODEL 1405-H MECHANICAL VACUUM PUMP

P_2 ; VEECO MODEL EP2-AB AIR COOLED OIL DIFFUSION PUMP

V_1, V_2 ; VEECO MODEL R-62S, 5/8", VACUUM VALVES

V_3 ; VEECO MODEL R-150S, 1 1/2", VACUUM VALVE

GA-1; HASTINGS-RAYDIST MODEL DV-3M THERMOCOUPLE GAUGE

GA-2; HASTINGS-RAYDIST MODEL DV-5M THERMOCOUPLE GAUGE

IND-1; HASTINGS-RAYDIST MODEL SV-1 INDICATOR (0 - 1000μ)

IND-2; HASTINGS-RAYDIST MODEL LV-1 INDICATOR (0 - 100μ)

A - A; CONNECTION TO VARIABLE (0 - 135 VAC) TRANSFORMER FOR DIFFUSION PUMP HEATER

B ; CONNECTION TO 115 VAC FOR COOLING BLOWER

FIGURE 4

HIGH VACUUM SYSTEM

which is fitted with a flange on each end. The diffusion pump output mates to one flange on this tube with an "O"-ring seal while the other flange is used as a seat for the "O"-ring seal of a cold trap finger which fits down inside the copper tube. A 1 1/2 inch Veeco vacuum valve is connected to the side of the cold trap tube, and the output side of this valve is joined to the pumpout tube on the Penning gauge with a 27 inch copper tube 1 1/2 inches ID. This length is used in order to clear the magnet. The forepressure manifold can be opened to the gauge system through a 5/8 inch Veeco vacuum valve. This permits the entire system to be pumped down to the required forepressure using the mechanical pump. The other side of the forepressure manifold connects to a 2000 cc ballast tank through another 5/8 inch vacuum valve. The ballast tank aids in maintaining proper forepressure to the diffusion pump while pumping the main system with the forepump. A thermocouple gauge is used to monitor forepressure. The useful pressure range for this gauge is from 10 to 1000 μ Hg. The gauge is mounted directly onto the forepressure manifold as shown in Fig. 4 . The high vacuum is monitored down to 10^{-3} mm Hg with another thermocouple gauge mounted at the end of the tubing which connects the vacuum system to the pumpout connection on the Penning gauge. Pressures in the gauge proper may be measured by calibrating it as a vacuum gauge.

Due to the "gettering" action of the Penning gauge,[11] and the need to adjust the gauge pressure above the minimum to which the diffusion pump will pump the system, a Granville Phillips model 9101-ML controlled leak is used. This leak is designed to have a leak rate continuously variable from 10 standard cm^3/sec to less than 10^{-10} standard cm^3/sec. The leak also provides a method of admitting gases other than air to the system.

Figure 5 is a schematic diagram of the high voltage power supply used. The circuit is a full wave voltage doubler using two 705 rectifier tubes. The power supply is part PP-93CPN-6 of radar set AN/CPN-6. The AC ripple component at 3000 volts was measured under no load conditions and found to be less than 5 volts AC. Current limiting is accomplished with a 300 K ohm, 200 watt power resistor in series with the high voltage output. This resistor provides a limiting current of 35 ma at full voltage output, well below the maximum output rating of the power supply (50 ma). A 0 to 1 ma meter is used with the 24 megohm filter resistor as a multiplier resistance to measure the voltage output. The current is continuously measured with a 0 to 10 ma meter while a 0 to 1 ma meter can be used by opening the shorting switch, SW_3. The positive high voltage is connected to the junction box with Belden #18018 high

---

[11] L. H. Martin and R. D. Hill, A Manual of Vacuum Practice, (Melbourne University Press, Melbourne, 1947), Chap. 2.

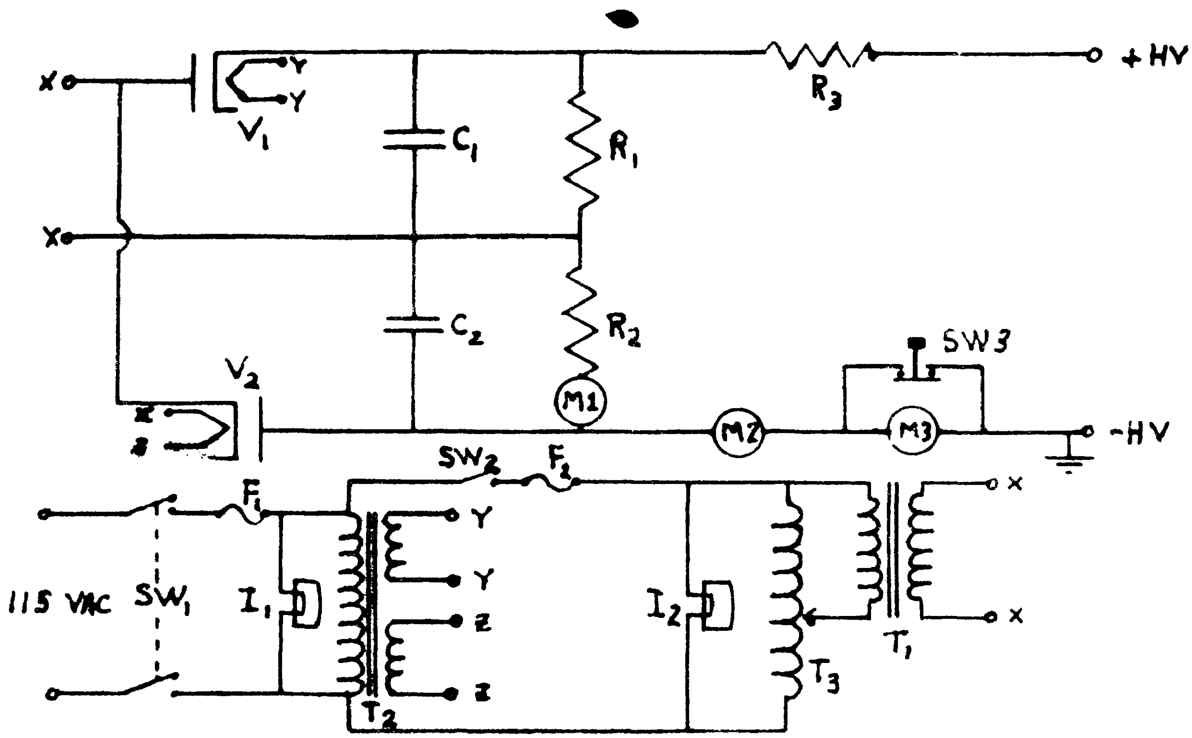

T_1; HIGH VOLTAGE TRANSFORMER, GALVIN #25C100471,
PRI: 115 VAC, 15 KVDC INS., SEC: 5600 VAC @ 100 ma

T_2; FILAMENT TRANSFORMER, GALVIN #25C100473, PRI: 115 VAC,
15 KVDC INS., TWO SEC: 5 VAC @ 5 A, 15 KVDC INS.

T_3; VARIABLE TRANSFORMER, PRI: 115 VAC, SEC: 0 - 135 VAC @ 3 A

V_1, V_2; WESTERN ELECTRIC TYPE 705

R_1, R_2; RESISTOR, COMPOSITION, HIGH VOLTAGE TYPE, 12 MEGOHM

R_3; RESISTOR, POWER, 300 K, 200 WATT

C_1, C_2; CAPACITOR, OIL FILLED, 1 mfd., @ 7500 VDC

M_1; VOLTMETER, 0 - 6 KVDC

M_2; MILLIAMMETER, 0 - 15 ma

M_3; MILLIAMMETER, 0 - 1 ma

SW_1; SWITCH, TOGGLE, DPST, 20 A @ 125 VAC

SW_2; SWITCH, TOGGLE, SPST, 8 A @ 125 VAC

SW_3; SWITCH, PUSHBUTTON, DPST, NC, 3 A @ 125 VAC

I_1, I_2; PILOT LAMP, NEON, GE TYPE 51

F_1, F_2; FUSE, BUSS TYPE MDE, 3 A @ 250 VAC

FIGURE 5, HIGH VOLTAGE POWER SUPPLY

voltage cable rated at 15 KV. Copper braid is pulled over the high voltage cable to provide shielding and a return circuit to the negative terminal of the supply.

The junction box serves a two fold purpose. Firstly, it provides mechanical support for the coupling of high voltage to the anode lead through a radio frequency choke made of 7 turns of #17 AWG copper wire, 1/2 inch in diameter and 1 inch long, and for the 1000 pf., 6KV ceramic disc blocking capacitor between the anode lead and the output to the receiver. Secondly, the junction box serves as a RF shield over the glass anode seal of the Penning gauge. The box is made of #17 B & S gauge copper and measures 4 x 5 x 5 inches. The front is a removable cover to allow access to the coupling connections to the anode lead. The box is soldered to the anode seal support tubing at a point adjacent to the anode seal.

A Navy RDO search receiver manufactured by the E. H. Scott Radio Company is used to detect oscillations. This receiver has a frequency range of 40 to 1000 mc using three separate tuning units. The signal from the first detector at the 30 mc IF frequency in the tuning unit is fed to a cathode follower stage in the receiver. The output of the cathode follower is terminated at the panoramic adaptor connector. A Panoramic Radio Products model SA-3 type T-2000 Panadaptor is used visually to inspect gauge oscillations detected by the RDO receiver. The IF of the Panadaptor is 30 mc while the sweep width and resolution are 2 mc and 20 kc, respectively. The stated sensitivity of the Panadaptor is 500 microvolts for a 1/4 inch baseline deflection.

PROCEDURE AND DATA

The procedure was to set the magnetic field at an arbitrary value and vary the high voltage until oscillations appeared on the Panadaptor when the receiver was tuned. It was noticed that a sharply defined peak in the current occurred for certain values of the anode voltage. This effect was useful in locating gauge oscillations at any new value of the magnetic field. This was done by varying the voltage until the peak in the current was observed. This voltage corresponded to the excitation voltage for a number of oscillations in the gauge, which were then observed on the panoramic adaptor by tuning the receiver through its range.

The magnetic field was measured with a Grassot fluxmeter and a flip coil. The fluxmeter was initially calibrated using a magnetron magnet whose field was measured with a TS-15A/AP gaussmeter. The gaussmeter had an accuracy of better than 1%, as determined using NMR techniques. By averaging several fluxmeter deflections for the same magnetic field, the error in the measurement of the magnetic fields used was estimated to be less than 2%.

For most runs, air was leaked into the system, and the gauge pressure was maintained at approximately 5×10^{-4} mm

Hg by pumping continuously against the controlled leak. One run was made using helium, but the results were not significantly different from those obtained with air.

In the dispersion relation, Eq. (31), the cavity modes are designated by the integers n, ℓ , m. The integer "n" denotes the order of the Bessel function which gives the radial dependence of the potential, "ℓ" denotes the number of the Bessel function zero corresponding to the surface of the cylinder, and "m" is the number of half wavelengths in one cylinder length. Since the anode ring must be an equipotential, the ring must either coincide with a node of oscillation or "n" must be zero. However, a node at the anode would not be observed since the anode potential would not vary. Thus, "n" has been set equal to zero. Only modes with an odd integral number of half wavelengths will have an antinode at the anode so "m" has been assigned odd integral values only. Under these conditions, the values of A for the three lowest modes may be calculated and are indicated on Fig. 1 by the notation 011, 021, and 013.

Table I contains a summary of the data which is also plotted in Fig. 1. The experimental points, designated by Δ and O, have been assigned to the lowest three modes predicted as described above, since one would expect the strongest oscillations to correspond to the lowest modes. All the points were taken for a pressure of 5×10^{-4} mm Hg.

TABLE I. Summary of representative data plotted in Fig. 1.

All of these measurements were made at the same pressure, approximately 0.5 microns Hg.

Cyclotron frequency f_c	Observed frequency f	Line width	F f/f_c	Anode kv.	Anode μA.	Mode assigned	Normalized propagation constant* A	Symbol
575 Mc.	142 Mc.	.02 Mc.	0.25	3.5	174	021	0.44	o
575	204	.02	0.36	3.5	174	011	1.01	●
575	297	.02	0.52	3.5	174	013	3.03	O
644	115	.02	0.18	2.9	215	021	0.44	△
644	165	.02	0.26	3.1	230	011	1.01	△
644	261	.5	0.41	2.9	235	013	3.03	△

* The normalized propagation constant, A, used here was calculated from our gauge dimensions using the formula in Eq. (31).

Using Eq. (9), the cyclotron frequency can be determined by the relation

$$f_c = \omega_c/2\pi = 2.80 \text{ mc/gauss.}$$

At the field strengths used for the data plotted in Fig. 1 this relation yields the cyclotron frequency as 575 mc at 205 gauss, and 644 mc at 230 gauss.

EXPERIMENTAL RESULTS AND CONCLUSIONS

The observed resonances show a marked dependence on the applied magnetic and electric fields. A pronounced variation in the gauge current was noticed to be concurrent with a change in the resonance amplitude and width. For a particular value of the magnetic field and pressure, the observed resonance lines could be pulled several megacycles by varying the high voltage. This variation in the frequency was also accompanied by a change in amplitude and/or width of the resonance.

It was observed that the discharge would not start at a value of the magnetic field less than 180 gauss if the pressure was set at 5×10^{-4} mm Hg and the voltage at 3.5 KV. Above this field strength, the rise in anode current was very abrubt attaining an initial value of approximately 160 μA when the discharge just starts with the field set at 190 gauss. Resonance lines were not observed when the gauge was just past the starting point for the discharge, but the oscillations seemed to appear quite suddenly as the magnetic field was increased.

As already mentioned, the gauge current was observed to peak sharply when the voltage was adjusted to maximum amplitude of certain oscillations. This correlation between resonance characteristics and gauge current implies that the oscillations are related to the conduction mechanism of the discharge.

The agreement between the calculated curves and the experimental points indicates that the observed resonances may be associated with the lowest slow wave modes in the cavity.

If the shape of the potential distribution from anode to cathode were a parabola, the frequency of oscillation for electrons about the potential maximum would be approximately 250 mc, while if the distribution were rectangular, a frequency of approximately 400 mc would be obtained. For the data plotted, the plasma frequency was approximately 300 mc. The relatively small difference between the observed oscillation frequency and the frequency of electron motion supports the possibility that the slow wave modes are excited by coupling between the electron beams and the plasma oscillations.

The enhanced conduction responsible for the current peak as a function of the voltage has been found to be associated with the behavior of the oscillations in the gauge. This implies that there is a connection between the oscillations and the conduction mechanism.

SUMMARY

After the discussion of the general construction of a Penning gauge and its characteristics, the lack of detailed theory on its operation has been cited. A derivation of the dielectric constant tensor, in which the interaction of the time-varying component of the magnetic field with the electrons has been neglected, was presented and used to derive the dispersion relation for slow wave modes in the quasi-static approximation for a plasma filled cylindrical cavity.

The prediction of observable modes of oscillation in the geometry used has been described. Experimentally observed oscillations have been shown to be assignable in an unambiguous fashion to the lowest three modes.

The current peaks as a function of the voltage were observed to correspond to changes in the oscillation amplitude and/or width. The characteristics of these peaks were not investigated thoroughly due to a lack of fine control of the high voltage supply.

The agreement between the calculated dispersion curves and the experimental data support the conclusion that the slow wave oscillations are associated with the conduction mechanism of the Penning gauge. The excitation

mechanism for these slow waves has been mentioned, and it seems likely that the interaction between the electron beams oscillating about the potential maximum and the plasma is able to excite oscillations as shown in reference 9.

The investigation performed is not complete; further work on the characteristics of slow wave oscillations in the Penning gauge, with particular emphasis on their role in the conduction mechanism, is planned. This more extensive investigation will be carried out by the group currently doing research along these lines under NASA research grant NsG 106-61.

BIBLIOGRAPHY

Backus, J., Characteristics of Electrical Discharges in Magnetic Fields, eds. A. Guthrie and R. K. Wakerling (McGraw-Hill Book Company, Inc., New York, 1949), Chap. 11. *(5)

Backus, J., J. Appl. Phys. 30, 1866 (1959) and J. Appl. Phys. 31, 400 (1960).

Bohm, D. and Gross, E. P., Phys. Rev. 75, 1851, 1864 (1949) and Phys. Rev. 79, 992 (1950). *(9)

Brown, S. C., Basic Data of Plasma Physics (John Wiley & Sons Inc., New York, 1959).

Chandrasekhar, S., Plasma Physics, comp. S.K. Trehan (The University of Chicago Press, Chicago, 1961), 3rd ed. *(7)

Drummond, J. E., Plasma Physics (McGraw-Hill Book Company, Inc., New York, 1961). *(3)

Dumas, G., Rev. Gen. de Elect. 64, 331 (1955).

Knauer, W., "Mechanism of the Penning Discharge at Low Pressures," Hughes Res. Rep. 223 (1961). *(6)

Martin, L. H. and Hill, R. D., A Manual of Vacuum Practice (Melbourne University Press, Melbourne, Austrailia, 1947). *(11)

Penning, F. M., Physica 4, 71 (1937). *(1)

Penning, F. M., Philips Tech. Rev. 2, 201 (1937).

Rose, D. J. and Clark, Jr., M., Plasmas and Controlled Fusion (The M.I.T. Press and John Wiley & Sons, Inc., New York, 1961).

Salz, F., Meyerand, Jr., R. G., Lary, E. C., and Walsh, A. P., Phys. Rev. Letters 6, 523 (1961). *(8)

Simpson, K. M., High Vacuum Equipment and Technique, eds. A. Guthrie and R. K. Wakerling (McGraw-Hill Book Company, Inc., New York, 1949), Chap. 3. *(4)

Thoneman, P. C., Progress in Nuclear Physics, ed. O. R. Frisch (Pergamon Press, Ltd., London, 1953), Vol. 3, Chap. 8. *(2)

Tonks, L. and Langmuir, I., Phys. Rev. 33, 1929.

Trivelpiece, A. W. and Gould, R. W., J. Appl. Phys. 30, 1784 (1959). *(10)

Wehner, G. K., Advances in Electronics and Electron Physics (Academic Press Inc., Publishers, New York, 1955), Vol. VII, p. 239 ff.

*( ) denotes footnoted reference.

VITA

Robert Newman Dennis, Jr.

Born in New York City, February 5, 1936. Attended Pelham Memorial High School, Pelham, New York and graduated from the Matthew Whaley School, Williamsburg, Virginia, 1954. Served four years in the U. S. Navy (1954-58). Graduated from the College of William and Mary in 1961 with the B.S. degree in physics.

In February 1961, the author entered the College of William and Mary as a graduate student in the department of physics under a NASA grant.